Electroluminescence from silicon-rich nitride/silicon superlattice structures

J. Warga,[1] R. Li,[1] S. N. Basu,[2,3] and L. Dal Negro[1,3,a)]
[1]*Department of Electrical and Computer Engineering, Boston University, Boston, Massachusetts 02215, USA*
[2]*Department of Mechanical Engineering, Boston University, Boston, Massachusetts 02215, USA*
[3]*Division of Materials Science and Engineering, Boston University, Boston, Massachusetts 02215, USA*

(Received 3 September 2008; accepted 30 September 2008; published online 17 October 2008)

Luminescent silicon-rich nitride/silicon superlattice structures (SRN/Si-SLs) with different silicon concentrations were fabricated by direct magnetron cosputtering deposition. Rapid thermal annealing at 700 °C resulted in the nucleation of small amorphous Si clusters that emit at 800 nm under both optical and electrical excitations. The electrical transport mechanism and the electroluminescence (EL) of SRN/Si-SLs have been investigated. Devices with low turn-on voltage (6 V) have been demonstrated and the EL mechanism has been attributed to bipolar recombination of electron-hole pairs at Si nanoclusters. Our results demonstrate that amorphous Si clusters in SRN/Si-SLs provide a promising route for the fabrication of Si-compatible optical devices. © *2008 American Institute of Physics*. [DOI: 10.1063/1.3003867]

Silicon nanocrystals embedded in silicon nitride matrices[1] provide an alternative approach, with respect to silicon oxide-based structures, in the fabrication of inexpensive light-emitting devices compatible with mainstream silicon technology. Light-emitting Si nanoclusters (Si-nc) dispersed in amorphous silicon nitride offer significant advantages over the more characterized oxide-based Si-nc systems. In particular, due to the low diffusivity of Si atoms in silicon nitride, thermally induced phase separation in silicon-rich nitride (SRN) results in a higher density of smaller Si clusters, which are predominantly amorphous. This amorphous nature deeply affects the optical emission properties of Si clusters in silicon nitride systems. In fact, the influence of surface states becomes predominant for small Si amorphous clusters below 3 nm in diameter,[2] and the probability of radiative recombination is enhanced due to nitrogen-related optical transitions spatially localized at the surface of the Si clusters.[3,4] It has recently been shown that SRN-based dielectrics give rise to intense near-infrared light emission with nanosecond-fast dynamics, small temperature quenching, and efficient energy transfer to Er ions.[3–6] In addition, the large effective refractive index of SRN-based nanostructures has led to the fabrication of high quality photonic crystals resonant structures.[5] Silicon nitride-based structures offer another important advantage over oxide-based active materials: a considerable reduction in the electron/hole injection barriers at the Si/silicon nitride interfaces, potentially resulting in the fabrication of low-voltage electroluminescent devices with improved electrical stability. Bulk SRN-based electroluminescent devices have been extensively studied and have resulted in turn-on voltages in the range of 8–15 V.[7,8] The electrical injection in SRN samples has been discussed according to several transport mechanisms, including Fowler–Nordheim[8,9] and trap-assisted tunnelling,[10] Poole–Frenkel conduction,[11] hopping, and space charge limited conduction (SCLC),[9,12,13] depending on sample quality (defect density), stoichiometry, and the injection field.

In this letter, we study light emission via optically and electrically excited amorphous Si clusters in SRN/Si superlattice structures (SRN/Si-SLs) fabricated by direct cosputtering[6] and we show that low turn-on voltages can be achieved when Si-nc form inside nanometer sized layers.

SRN/Si-SLs samples with 400 nm total thickness were fabricated on Si substrates by radio frequency magnetron cosputtering from Si and Si_3N_4 targets and annealed using a rapid thermal annealing furnace in N_2/H_2 forming gas (5% hydrogen) for 10 min at a temperature of 700 °C, which was found to maximize the photoluminescence (PL) signal.[3–6] The sputtering was performed in a Denton Discovery 18 confocal-target sputtering system, as described elsewhere.[5] Transparent indium tin oxide (ITO) top contacts were lithographically defined and deposited by radio frequency magnetron sputtering from an ITO target. Aluminum (Al) was evaporated on the back surface and used as a cathode. The current-voltage (J-V) characteristics of the devices were measured under forward bias condition at room temperature by using a HP4155A semiconductor parameter analyzer. The atomic concentrations of Si and N in the deposited films were measured, within 0.5% accuracy, with energy dispersive x-ray (EDX) analysis (Oxford ISIS). Room temperature electroluminescence (EL) was measured under forward bias using a Keithley 2400-LV sourcemeter. Steady-state room temperature PL was excited using the 488 nm line of an Ar pump laser (Spectra Physics, 177–602). EL and PL were detected using a photomultiplier tube (Oriel 77348). All EL and PL spectra have been accurately corrected by the spectral response of the PL setup. The film microstructure was characterized by transmission electron microscopy (TEM).

Figure 1 shows a TEM bright-field image of a representative SRN/Si-SLs sample in cross section, taken using a JEOL 2010 TEM operated at 200 kV. The structure has been annealed at 700 °C for 10 min and contains 47% Si, as measured by EDX. The average Si and SRN layer thicknesses of the SRN/Si-SLs sample were measured to be 3.4 and 4.2 nm, respectively. In the inset of Fig. 1, Si nanoclusters can be seen in the SRN layers, as indicated by arrows. The Si clus-

[a)]Author to whom correspondence should be addressed. Electronic mail: dalnegro@bu.edu.

 © 2008 American Institute of Physics

Downloaded 11 Feb 2009 to 128.197.27.9. Redistribution subject to AIP license or copyright; see http://apl.aip.org/apl/copyright.jsp

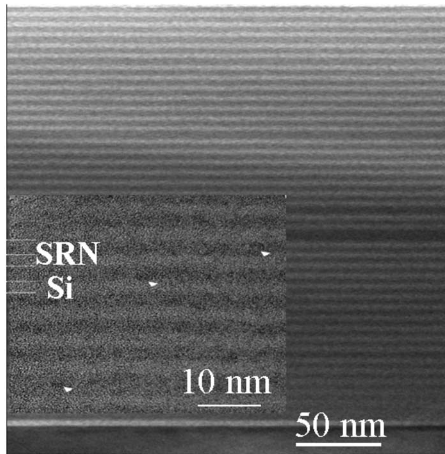

FIG. 1. Bright-field TEM cross-section micrograph of a representative SRN/Si-SLs fabricated by direct cosputtering. Inset: high-resolution TEM cross section of a portion of the same SRN/Si-SLs showing Si-nc (indicated by arrows).

ters are amorphous with an average diameter of ~2.5 nm.

In order to understand the origin of the EL in the SRN/Si-SLs samples, we start by discussing the behavior of the PL for samples deposited with different silicon concentrations. Figure 2(a) shows the room temperature PL spectra of the SRN/Si-SLs samples, which consist of broad near-infrared bands centered at around 800 nm. However, in the sample with 50% silicon concentration we observed a PL spectrum centered at around 650 nm, which is known to originate from defect states in silicon nitride.[14] In the inset of Fig. 2(a), we show the integrated PL signal from 400 to 850 nm. We have found that the PL in SRN/Si-SLs samples is maximized for an optimum silicon concentration equal to 53%.

Using these samples, we fabricated electrical device structures for the study of the electrical injection mechanism and EL in SRN/Si-SLs under direct current injection. The inset of Fig. 2(b) shows the schematic of the electrical device structure. For the SLs, layers were deposited alternating between SRN and Si on a *p*-type Si substrate. After annealing of the active layer, ITO contacts of 1 mm^2 were lithographically defined and deposited via direct sputtering on top. Then an Al back contact was evaporated onto the *p*-type Si substrate. *J-V* and EL measurements were taken by positively biasing the *p*-type Si substrate.

In Fig. 2(b) we show the *J-V* characteristic (open circles) measured at room temperature on the best-emitting electrical structure consisting of SRN/Si-SLs with 53% silicon concentration. In order to identify the charge transport mechanism in SRN/Si-SLs, we attempted to fit the experimental *J-V* data to all the mechanistic models on silicon nitride proposed in the literature. In particular, those models include SCLC (solid), direct tunneling (dot), Fowler–Nordheim tunneling (dash), Frenkel–Poole emission (dash dot), and Ohmic (dash dot dot) conduction (hopping), all of which have two free fitting parameters except Ohmic (which has only one). Figure 2(b) shows that, within the investigated voltage range, our experimental data are best fitted, over almost six orders of magnitude, by a power law $J \sim V^m$, where $m=2.3$. This model is known to describe SCLC with a distribution of traps characterized by a *J-V* relation,[9,12,13]

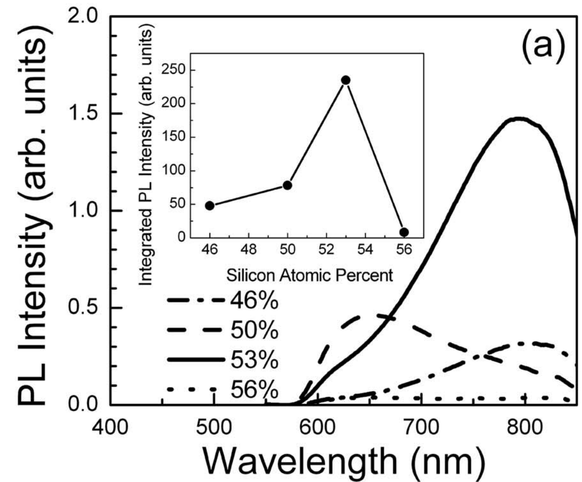

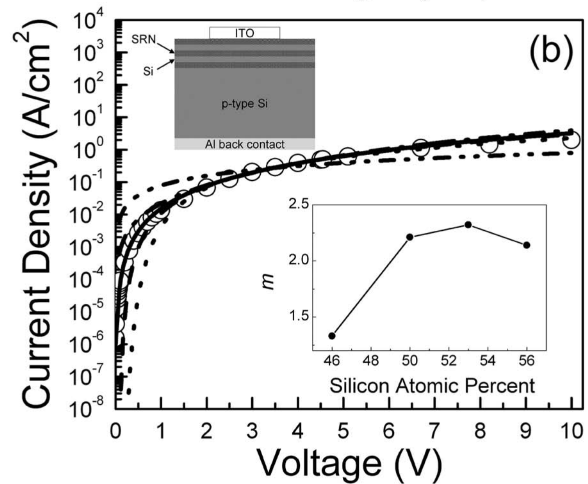

FIG. 2. (a) PL spectra of SRN/Si-SLs with different atomic percent Si. Inset shows integrated PL intensities of SRN/Si-SLs samples for stoichiometry varied from 46% to 56% atomic Si. (b) Experimental *J-V* characteristic (open circles) of the sample with 53% atomic Si. Data were fitted by $J=A_1V^m$ for SCLC (solid), $J=A_2V\exp(-b_2/V)$ for direct tunneling (dot), $J=A_3V^2\exp(-b_3/V)$ for Fowler–Nordheim tunneling (dash), $J=A_4V\exp(b_4V^{1/2})$ for Frenkel–Poole emission (dash dot), and $J=A_5V$ for Ohmic (dash dot dot), where A_i and b_i are the fitting parameters. The bottom right inset shows the variation in the *m* parameter with the silicon concentration. The schematic of the electrical device structures is shown in the upper inset.

$$J=\frac{9\varepsilon\mu V^m}{8d^3},$$

where d, ε, and μ are the thickness, dielectric constant, and drift mobility of the SRN film, respectively, and the exponent m characterizes the energy width of the trap distribution. Current data of other Si content samples are fit with SCLC, which yields m values in the range from 1.3 to 2.3 by increasing the Si content (Fig. 2 inset). Based on this fit, we can estimate drift mobility in the SRN layer between 10^{-3} and 10^{-4} cm^2/V s, in agreement with published literature.[15]

It is important to keep in mind that for such small drift mobilities[16,17] high electric fields in excess of 1 MV/cm are needed in order to generate electron-hole pairs by impact ionization. On the other hand, we obtain a conservative estimate for the injection electric field in our devices by assuming that all the voltage drops across the mostly insulating SRN active layers of the SRN/Si-SLs. Considering a total SRN layer thickness of 200 nm, we obtain an electric field of about 50 kV/cm, which is much smaller than what is neces-

Downloaded 11 Feb 2009 to 128.197.27.9. Redistribution subject to AIP license or copyright; see http://apl.aip.org/apl/copyright.jsp

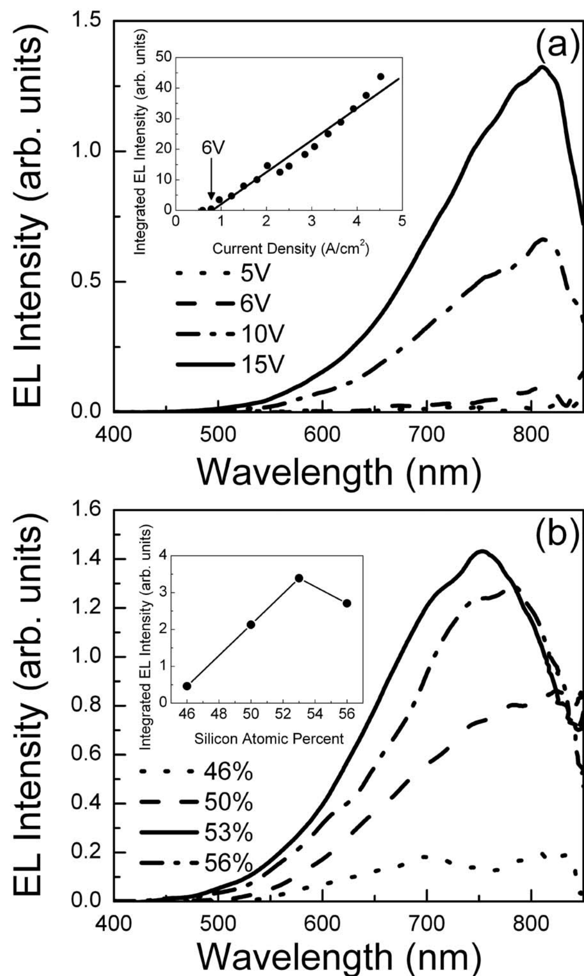

FIG. 3. (a) EL spectra at varied voltages. Inset shows linear relation between integrated EL intensity and current density with a turn-on voltage of 6 V. (b) EL spectra of SRN/Si-SLs with different atomic percent Si measured at 10 V. The inset shows the integrated EL intensities of SRN/Si-SLs samples with stoichiometry varying from 46% to 56% atomic Si.

sary for impact ionization. Therefore, we tested the possibility of EL occurring at low injection fields in SLs.

In Fig. 3 we summarize the EL results obtained on the SRN/Si-SLs device structures. In Fig. 3(a) the EL emission is shown for increasing voltages. The EL spectrum becomes clearly detectable at a low turn-on voltage of 6 V (at 0.78 A/cm^2). We notice that as the voltage is increased to 15 V, the EL spectra do not show any frequency shift. In addition, the inset of Fig. 3(a) shows a linear dependence of the integrated EL (from 400 to 850 nm) intensity with respect to the injection current density. This linear behavior is consistent with low-field bipolar injection rather than impact ionization at the emitting nanoclusters, which would result in a super-linear dependence. We know that in the case of impact excitation, a broadening of the EL spectrum is observed as the current density increases, due to the hot electrons excitation of Si-nc with progressively larger bandgaps, which emit at shorter wavelengths. In addition, more than one electron-hole pair is created by one hot electron during impact excitation, leading to nonlinear integrated EL versus J characteristics. The observed linearity of the integrated EL with current density characteristic of the SRN/Si-SLs combined with the absence of EL spectral changes suggest a one to one correlation between injected carriers and excited Si-nc in the active layer, which is consistent with bipolar electron-hole pair recombination.[18]

Next, we compared the light emission under optical and electrical pumpings for the same set of samples. Figure 3(b) shows the EL data for samples with different silicon content. Negligible spectral shift is observed between the EL and PL line shapes, although spectral shift is observed only for the sample containing 50% atomic silicon. In fact, defects in silicon nitride have a significantly smaller electrical pumping cross section than silicon clusters.[14] In Fig. 2(a) there is a band at 650 nm for the 50% silicon sample, which is not excited in the same sample under electrical pumping as shown in Fig. 3(b). The inset of Fig. 3(b) shows the behavior of the integrated EL intensity for different silicon concentrations in the superlattices. We notice that the optimization of the EL signal follows directly that of the PL, showing that in these structures both PL and EL originate from the same luminescent centers.

In conclusion, we studied the PL and the electroluminescence behaviors of SRN/Si-SLs structures obtained by direct cosputtering followed by rapid thermal annealing. Samples of different silicon concentrations have been fabricated along with corresponding electrical device structures. We have demonstrated low turn-on voltage (6 V) EL occurring at low injection fields and we showed that both the PL and the EL originate from bipolar electron-hole injection in small silicon clusters.

This work was partially supported by the U.S. Air Force MURI program on “Electrically-Pumped Silicon-Based Lasers for Chip-Scale Nanophotonic Systems” supervised by Dr. Gernot Pomrenke.

[1]N. M. Park, C. J. Choi, T. Y. Seong, and S. J. Park, Phys. Rev. Lett. **86**, 1355 (2001).
[2]A. J. Williamson, J. C. Grossman, R. Q. Hood, A. Puzder, and G. Galli, Phys. Rev. Lett. **89**, 196803 (2002).
[3]L. Dal Negro, J. H. Yi, L. C. Kimerling, S. Hamel, A. Williamson, and G. Galli, Appl. Phys. Lett. **88**, 183103 (2006).
[4]L. Dal Negro, J. H. Yi, J. Michel, L. C. Kimerling, T.-W. F. Chang, V. Sukhovatkin, and E. H. Sargent, Appl. Phys. Lett. **88**, 233109 (2006).
[5]M. Makarova, V. Sih, J. Warga, R. Li, L. Dal Negro, and J. Vuckovic, Appl. Phys. Lett. **92**, 161107 (2008).
[6]L. Dal Negro, R. Li, J. Warga, and S. N. Basu, Appl. Phys. Lett. **92**, 181105 (2008).
[7]Z. Pei, Y. R. Chang, and H. L. Hwang, Appl. Phys. Lett. **80**, 2839 (2002).
[8]R. Huang, K. Chen, H. Dong, D. Wang, H. Dong, W. Li, J. Xu, Z. Ma, and L. Xu, Appl. Phys. Lett. **91**, 111104 (2007).
[9]S. A. Awan, R. D. Gould, and S. Gravano, Thin Solid Films **355**, 456 (1999).
[10]S. Fleischer, P. T. Lai, and Y. C. Cheng, J. Appl. Phys. **72**, 5711 (1992).
[11]S. Habermehl and C. Carmignani, Appl. Phys. Lett. **80**, 261 (2002).
[12]F. Chen, B. Li, R. A. Dufresne, and R. Jammy, J. Appl. Phys. **90**, 1898 (2001).
[13]M. Vila, C. Prieto, and R. Ramirez, Thin Solid Films **459**, 195 (2004).
[14]S. V. Deshpande, E. Gulari, S. W. Brown, and S. C. Rand, J. Appl. Phys. **77**, 6534 (1995).
[15]R. Hattori and J. Shirafuji, Appl. Phys. Lett. **54**, 1118 (1989).
[16]R. A. M. Hikmet, D. V. Talapin, and H. Weller, J. Appl. Phys. **93**, 3509 (2003).
[17]Z. Pei, A. Y. K. Su, H. L. Hwang, and H. L. Hsiao, Appl. Phys. Lett. **86**, 063503 (2005).
[18]K. S. Cho, N. M. Park, T. Y. Kim, K. H. Kim, G. Y. Sung, and J. H. Shin, Appl. Phys. Lett. **86**, 071909 (2005).

Downloaded 11 Feb 2009 to 128.197.27.9. Redistribution subject to AIP license or copyright; see http://apl.aip.org/apl/copyright.jsp